

# Dispersive calculation of complex Regge trajectories for the lightest $f_2$ resonances

J.A. Carrasco,<sup>1</sup> J. Nebreda,<sup>1,2</sup> J.R. Pelaez,<sup>1</sup> and A.P. Szczepaniak<sup>3,4,5</sup>

<sup>1</sup>*Departamento de Física Teórica II, Universidad Complutense de Madrid, 28040 Madrid, Spain*

<sup>2</sup>*Yukawa Institute for Theoretical Physics, Kyoto University, 606-8502 Kyoto, Japan*

<sup>3</sup>*Physics Department Indiana University, Bloomington, IN 47405, USA*

<sup>4</sup>*Center for Exploration of Energy and Matter, Indiana University, Bloomington, IN 47403, USA*

<sup>5</sup>*Thomas Jefferson National Accelerator Facility, Newport News, VA 23606, USA*

(Dated: October 19, 2018)

We apply a recently developed dispersive formalism to calculate the Regge trajectories of the  $f_2(1270)$  and  $f_2'(1525)$  mesons. Trajectories are calculated, not fitted to a family of resonances. Assuming that these spin-2 resonances can be treated in the elastic approximation the only input are the pole position and residue of the resonances. In both cases, the predicted Regge trajectories are almost real and linear, with slopes in agreement with the universal value of order  $1 \text{ GeV}^{-2}$ .

## I. INTRODUCTION

There is growing evidence for the existence of non-ordinary hadrons that do not follow the quark model, *i.e.* the quark-antiquark-meson or three-quark-baryon classification. Meson Regge trajectories relate resonance spins  $J$  to the square of their masses and for ordinary mesons they are approximately linear. The functional form of a Regge trajectory depends on the underlying dynamics and, for example, the linear trajectory for mesons is consistent with the quark model as it can be explained in terms of a rotating relativistic flux tube that connects the quark with the antiquark. Regge trajectories associated with non-ordinary mesons do not, however, have to be linear. The non-ordinary nature of the lightest scalar meson, the  $f_0(500)$  also referred to as the  $\sigma$ , together with a few other scalars, has been postulated long ago [3]. In the context of the Regge classification, in a recent study of the meson spectrum in [1] it was concluded that the  $\sigma$  meson does not belong to the same set of trajectories that many ordinary mesons do. In [2], it was concluded that the  $\sigma$  can be omitted from the fits to linear  $(J, M^2)$  trajectories because of its large width. The reason is that its width was taken as measure of the uncertainty on its mass and it was found that, when fitting trajectory parameters, its contribution to the overall  $\chi^2$  was insignificant.

In a recent work [4] we developed a formalism based on dispersion relations that, instead of fitting a specific, *e.g.* linear, form to spins and masses of various resonances, enables us to calculate the trajectory using as input the position and the residue of a complex resonance pole in a scattering amplitude. When the method was applied to the  $\rho(770)$  resonance, which appears as a pole in the elastic  $P$ -wave  $\pi\pi$  scattering, the resulting trajectory was found to be, to a good approximation, linear. The resulting slope and intercept are in a good agreement with phenomenological Regge fits. The slope, which is slightly less than  $1 \text{ GeV}^{-2}$ , is expected to be universal for all ordinary trajectories. It is worth noting that in this approach the resonance width is, as it should be, related to the imaginary part of the trajectory and not a source of an uncertainty. The  $\sigma$  meson also appears as a pole in the  $\pi\pi$   $S$ -wave scattering. The position and residue of the pole has recently been accurately determined in [5] using rigorous dispersive formalisms. When the same method was applied to the  $\sigma$  meson, however, we found quite a different trajectory. It has a significantly larger imaginary part and the slope parameter, computed at the physical mass as a derivative of the spin with respect to the mass squared, is more than one order of magnitude smaller than the universal slope. The trajectory is far from linear, instead it is qualitatively similar to a trajectory of a Yukawa potential. We also note that deviation from linearity is not necessarily implied by the large width of the  $\sigma$  since it was also shown in [4] that resonances with large widths may belong to linear trajectories. Our findings give further support for the non-ordinary nature of the  $\sigma$ .

Still, one may wonder if the single case of the  $\rho$  meson, where the method agrees with Regge phenomenology, gives sufficient evidence that it can distinguish between ordinary and non-ordinary mesons. In this letter, therefore we show that other ordinary trajectories can be predicted with the same technique, as long as the underlying resonances are almost elastic. For this purpose, we have concentrated on resonances that decay nearly 100% to two mesons. In addition to the  $\rho$  there are two other well-known examples: the  $f_2(1270)$ , whose branching ratio to  $\pi\pi$  is  $84.8_{-1.2}^{+2.4}\%$ , and the  $f_2'(1525)$ , with branching ratio to  $K\bar{K}$  of  $(88.7 \pm 2.2)\%$ . These resonances are well established in the quark model and as we show below, Regge trajectories predicted by our method come out almost real and linear with a slope close to the universal one. There is an additional check on the method that we perform here. Since the formalism used in the case of the  $\rho$  was based on a twice-subtracted dispersion relation, the trajectory had a linear term plus a dispersive integral over the imaginary part. Since the imaginary part of the trajectory is closely related to the decay width, one might wonder if the  $\rho(770)$ ,  $f_2(1270)$  and  $f_2'(1525)$  trajectories come out straight just because their widths are small. In other words, that for narrow resonances, the straight line behavior is not predicted but it is already

built in through subtractions. For this reason, in this work, we also consider three subtractions and show that for the ordinary resonances under study the quadratic term is negligible.

The paper is organized as follows. In the next section we briefly review the dispersive method and in Sect.III we present the numerical results. In Sect.IV we discuss results of the calculation with three subtractions. Summary and outlook are given in Sect.V.

## II. DISPERSIVE DETERMINATION OF A REGGE TRAJECTORY FROM A SINGLE POLE

The partial wave expansion of the elastic scattering amplitude,  $T(s, t)$ , of two spinless mesons of mass  $m$  is given by

$$T(s, t) = 32K\pi \sum_l (2l+1)t_l(s)P_l(z_s(t)), \quad (1)$$

where  $z_s(t)$  is the s-channel scattering angle and  $K = 1, 2$  depending on whether the two mesons are distinguishable or not. The partial waves  $t_l(s)$  are normalized according to

$$t_l(s) = e^{i\delta_l(s)} \sin \delta_l(s) / \rho(s), \quad \rho(s) = \sqrt{1 - 4m^2/s}, \quad (2)$$

where  $\delta_l(s)$  is the phase shift. The unitarity condition on the real axis in the elastic region,

$$\text{Im}t_l(s) = \rho(s)|t_l(s)|^2, \quad (3)$$

is automatically satisfied. When  $t_l(s)$  is continued from the real axis to the entire complex plane, unitarity determines the amplitude discontinuity across the cut on the real axis above  $s = 4m^2$ . It also determines the continuation in  $s$ , at fixed  $l$ , onto the second sheet where resonance poles are located. It follows from Regge theory that the same resonance poles appear when the amplitude is continued into the complex  $l$ -plane [6], leading to

$$t_l(s) = \frac{\beta(s)}{l - \alpha(s)} + f(l, s), \quad (4)$$

where  $f(l, s)$  is analytical near  $l = \alpha(s)$ . The Regge trajectory  $\alpha(s)$  and residue  $\beta(s)$  satisfy  $\alpha(s^*) = \alpha^*(s)$ ,  $\beta(s^*) = \beta^*(s)$ , in the complex- $s$  plane cut along the real axis for  $s > 4m^2$ . Thus, as long as the pole dominates in Eq.(4), partial wave unitarity, Eq.(3), analytically continued to complex  $l$  implies,

$$\text{Im} \alpha(s) = \rho(s)\beta(s), \quad (5)$$

and determines the analytic continuation of  $\alpha(s)$  to the complex plane [8]. At threshold, partial waves behave as  $t_l(s) \propto q^{2l}$ , where  $q^2 = s/4 - m^2$ , so that if the Regge pole dominates the amplitude, we must have  $\beta(s) \propto q^{2\alpha(s)}$ . Moreover, following Eq.(1), the Regge pole contribution to the full amplitude is proportional to  $(2\alpha + 1)P_\alpha(z_s)$ , so that in order to cancel poles of the Legendre function  $P_\alpha(z_s) \propto \Gamma(\alpha + 1/2)$  the residue has to vanish when  $\alpha + 3/2$  is a negative integer, *i.e.*,

$$\beta(s) = \gamma(s)\hat{s}^{\alpha(s)}/\Gamma(\alpha(s) + 3/2). \quad (6)$$

Here we defined  $\hat{s} = (s - 4m^2)/s_0$  and introduced a scale  $s_0$  to have the right dimensions. The so-called reduced residue,  $\gamma(s)$ , is a real analytic function. Hence, on the real axis above threshold, since  $\beta(s)$  is real, the phase of  $\gamma$  is

$$\arg \gamma(s) = -\text{Im}\alpha(s) \log(\hat{s}) + \arg \Gamma(\alpha(s) + 3/2). \quad (7)$$

Consequently, we can write for  $\gamma(s)$  a dispersion relation:

$$\gamma(s) = P(s) \exp \left( c_0 + c's + \frac{s}{\pi} \int_{4m^2}^{\infty} ds' \frac{\arg \gamma(s')}{s'(s' - s)} \right), \quad (8)$$

where  $P(s)$  is an entire function. Note that the behavior at large  $s$  cannot be determined from first principles, but, as we expect linear Regge trajectories for ordinary mesons, we should allow  $\alpha$  to behave as a first order polynomial at large- $s$ . This implies that  $\text{Im}\alpha(s)$  decreases with growing  $s$  and thus it obeys the dispersion relation [6, 7]:

$$\alpha(s) = \alpha_0 + \alpha's + \frac{s}{\pi} \int_{4m^2}^{\infty} ds' \frac{\text{Im}\alpha(s')}{s'(s' - s)}. \quad (9)$$

Assuming  $\alpha' \neq 0$ , from unitarity, Eq.(5), in order to match the asymptotic behavior of  $\beta(s)$  and  $\text{Im}\alpha(s)$  it is required that  $c' = \alpha'(\log(\alpha's_0) - 1)$  and that  $P(s)$  can at most be a constant,  $P(s) = \text{const.}$  Therefore, using Eq.(4), we arrive at the following three equations, which define the ‘‘constrained Regge-pole’’ amplitude [8]:

$$\text{Re } \alpha(s) = \alpha_0 + \alpha' s + \frac{s}{\pi} PV \int_{4m^2}^{\infty} ds' \frac{\text{Im}\alpha(s')}{s'(s' - s)}, \quad (10)$$

$$\text{Im } \alpha(s) = \frac{\rho(s)b_0 \hat{s}^{\alpha_0 + \alpha' s}}{|\Gamma(\alpha(s) + \frac{3}{2})|} \exp\left(-\alpha' s[1 - \log(\alpha' s_0)] + \frac{s}{\pi} PV \int_{4m^2}^{\infty} ds' \frac{\text{Im}\alpha(s') \log \frac{\hat{s}}{s'} + \arg \Gamma(\alpha(s') + \frac{3}{2})}{s'(s' - s)}\right), \quad (11)$$

$$\beta(s) = \frac{b_0 \hat{s}^{\alpha_0 + \alpha' s}}{\Gamma(\alpha(s) + \frac{3}{2})} \exp\left(-\alpha' s[1 - \log(\alpha' s_0)] + \frac{s}{\pi} \int_{4m^2}^{\infty} ds' \frac{\text{Im}\alpha(s') \log \frac{\hat{s}}{s'} + \arg \Gamma(\alpha(s') + \frac{3}{2})}{s'(s' - s)}\right), \quad (12)$$

where  $PV$  denotes the principal value. For real  $s$ , the last two equations reduce to Eq.(5). The three equations are solved numerically with the free parameters fixed by demanding that the pole on the second sheet of the amplitude in Eq. (4) is at a given location. Thus we will be able to obtain the two independent trajectories corresponding to the  $f_2(1270)$  and  $f'_2(1525)$  resonances from their respective pole parameters. Note that we are not imposing, but just allowing, linear trajectories.

### III. NUMERICAL RESULTS

In principle, the method described in the previous section is suitable for resonances that appear in the elastic scattering amplitude, *i.e.* they only decay to one two-body channel. For simplicity we are also focusing on cases where the two mesons in the scattering state have the same mass. We assume that both the  $f_2(1270)$  and the  $f'_2(1525)$  resonances can be treated as purely elastic and we will use their decay fractions into channels other than  $\pi\pi$  and  $K\bar{K}$ , respectively, as an additional systematic uncertainty in their widths and couplings. In our numerical analysis we fit the pole,  $s_p$ , and residue,  $|g^2|$ , found in the second Riemann sheet of the Regge amplitude. In this amplitude the  $\alpha(s)$  and  $\beta(s)$  are constrained to satisfy the dispersion relations in Eqs.(11) and (12). Thus, the fit determines the parameters  $\alpha_0, \alpha', b_0$  for the trajectory of each resonance. In practice, we minimize the sum of squared differences between the input and output values for the real and imaginary parts of the pole position and for the absolute value of the squared coupling, divided by the square of the corresponding uncertainties. At each step in the minimization procedure a set of  $\alpha_0, \alpha'$  and  $b_0$  parameters is chosen and the system of Eqs.(10) and (11) is solved iteratively. The resulting Regge amplitude for each  $\alpha_0, \alpha'$  and  $b_0$  is then continued to the complex plane, in order to determine the resonance pole in the second Riemann sheet, and the  $\chi^2$  is calculated by comparing this pole to the corresponding input.

#### A. $f_2(1270)$ resonance

In the case of the  $f_2(1270)$  resonance, we use as input the pole obtained from the conformal parameterization of the D0 wave from Ref [9]. In that work the authors use different parameterizations in different regions of energy and impose a matching condition. Here we will use the parameterization valid in the region where the resonance dominates the scattering amplitude, namely, in the interval  $2m_K \leq s^{1/2} \leq 1420$  MeV. Moreover, we will decrease the width down to 85% of the value found in [9] to account for the inelastic channels. The conformal parameterization results in the pole located at

$$\sqrt{s_{f_2}} = M - i\Gamma/2 = 1267.3_{-0.9}^{+0.8} - i(87 \pm 9) \text{ MeV}$$

and a coupling of

$$|g_{f_2\pi\pi}|^2 = 25 \pm 3 \text{ GeV}^{-2}.$$

With these input parameters, we follow the minimization procedure as explained above, until we get a Regge pole at  $\sqrt{s_{f_2}} = (1267.3 \pm 0.9) - i(89 \pm 10)$  MeV and coupling  $|g_{f_2\pi\pi}|^2 = 25 \pm 3 \text{ GeV}^{-2}$ . In Fig. 1 we show the corresponding constrained Regge-pole amplitude on the real axis versus the conformal parameterization that was constrained by the data [9]. This comparison is a check that our Regge-pole amplitude, which neglects the background  $f(l, s)$  term in Eq.(4), describes well the amplitude in the pole region, namely for  $(M - \Gamma/2)^2 < s < (M + \Gamma/2)^2$ . The grey bands cover the uncertainties arising from the errors of the input and include an additional 15% systematic uncertainty in

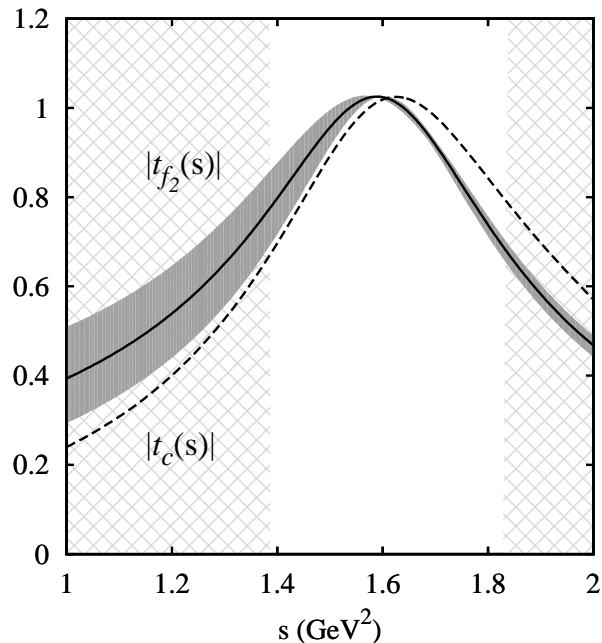


FIG. 1: The solid line represents the absolute value of the constrained Regge-pole amplitude for the  $f_2(1270)$  resonance. The gray bands cover the uncertainties due to the errors in the input pole parameters. The dashed line corresponds to the absolute value of the data fit obtained in [9]. Let us recall that only the parameters of the pole given by this parameterization have been used as input, and not the amplitude itself. The regions covered with a mesh correspond to  $s < (M - \Gamma/2)^2$  and  $s > (M + \Gamma/2)^2$ , where the background might not be negligible anymore.

the width as explained above. Taking into account that only parameters of the pole have been fitted, but not the whole amplitude in the real axis, and that we have completely neglected the background in Eq. (4), the agreement between the two amplitude models is very good, particularly in the resonance region. Of course, the agreement deteriorates as we move away from the peak region as illustrated by the shadowed energy regions  $s < (M - \Gamma/2)^2$  and  $s > (M + \Gamma/2)^2$ .

Since our constrained Regge amplitude provides a good description of the resonance region we can trust the resulting Regge trajectory. The parameters of the trajectory obtained through our minimization procedure are as follows,

$$\alpha_0 = 0.9_{-0.3}^{+0.2}; \quad \alpha' = 0.7_{-0.2}^{+0.3} \text{ GeV}^{-2}; \quad b_0 = 1.3_{-0.8}^{+1.4}. \quad (13)$$

In Fig. 2 we show the real and imaginary parts of  $\alpha(s)$ , with solid and dashed lines, respectively. Again, the gray bands cover the uncertainties coming from the errors in the input pole parameters. We find that the real part of the trajectory is almost linear and much bigger than the imaginary part. It is as expected for Regge trajectories of ordinary mesons. For comparison, we also show, with a dotted line, the Regge trajectory obtained in [1] by fitting a Regge linear trajectory to the meson states associated with  $f_2(1270)$ , which is traditionally referred to as the  $P'$  trajectory. We see that the two trajectories are in good agreement. Indeed, our parameters are compatible, within errors, with those in [1]:  $\alpha_{P'} \approx 0.71$  and  $\alpha'_{P'} \approx 0.83 \text{ GeV}^{-2}$ . We also include in Fig. 2 the resonances from the PDG [10] listing that could be associated with this trajectory.

In Fig. 2 the trajectory has been extrapolated to high energies, where the elastic approximation does not hold any more and we cannot hope to give a precise prediction for its behavior. The only reason to do this is to show the position of the candidate states connected to the  $f_2(1270)$ . In the figure, this region is covered with a mesh to the right from the line at the  $s$  that corresponds to the resonance mass plus three half-widths. Of course, we cannot confirm which of these resonances belongs to the  $f_2(1270)$  trajectory, but we observe that the  $J = 4$  resonance could be the  $f_4(2050)$ , as proposed in [1], or the  $f_J(2220)$  [11] or even the  $f_4(2300)$ . All these resonances appear in the PDG, but are omitted from the summary tables.

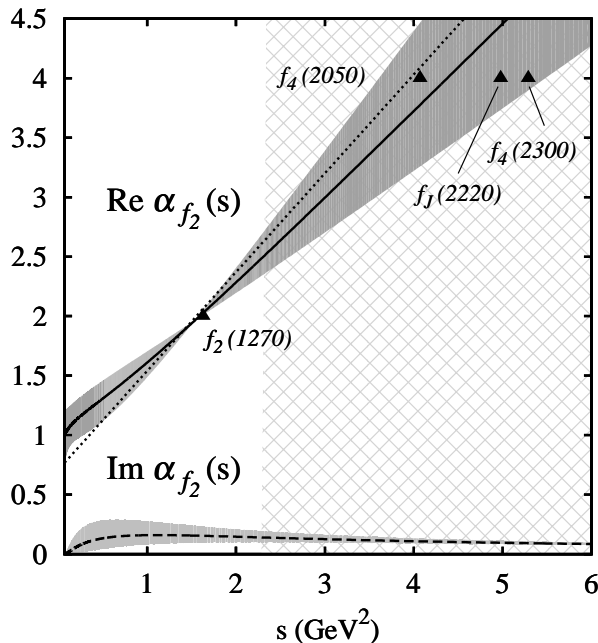


FIG. 2: Real (solid) and imaginary (dashed) parts of the  $f_2(1270)$  Regge trajectory. The gray bands cover the uncertainties due to the errors in the input pole parameters. The area covered with a mesh is the mass region starting three half-widths above the resonance mass, where our elastic approach should be considered only as a mere extrapolation. For comparison, we show with a dotted line the  $f_2(1270)$  Regge trajectory obtained in [1], traditionally called the  $P'$  trajectory. We also show the resonances listed in the PDG that are candidates for this trajectory. Note that their average mass does not always coincide with the nominal one, as is the case for the  $f_2(1270)$ .

### B. $f'_2(1525)$ resonance

As commented above, the  $f'_2(1525)$  decays mainly to two kaons. Although there is no scattering data on the  $l = 2$  elastic  $\bar{K}K$  phase shift in this mass region, the mass and width of the  $f'_2(1525)$  are given in the PDG [10]. Thus we use  $M_{f'_2} = 1525 \pm 5$  MeV and  $\Gamma_{f'_2}^{KK} = 69^{+10}_{-9}$  MeV, where the central value of this width corresponds to the decay into  $\bar{K}K$  only. Now, we infer the scattering pole parameters assuming the  $f'_2(1525)$  is well described by an elastic Breit-Wigner shape, so that we take the pole to be at  $s_{f'_2} = (M_{f'_2} - i\Gamma_{f'_2}/2)^2$  and the residue to be  $\text{Res} = -M_{f'_2}^2 \Gamma_{f'_2}^{KK} / 2p$ , where  $p$  is the CM momenta of the two kaons. Since  $|g|^2 = -16\pi(2l+1)\text{Res}/(2p)^{2l}$ , we find  $|g_{f'_2 KK}|^2 = 19 \pm 3$  GeV $^{-2}$ .

With these input parameters we solve the dispersion relations using the same minimization method and obtain the following Regge pole parameters:  $\sqrt{s_{f'_2}} = (1525 \pm 5) - i(34^{+4}_{-5})$  MeV and  $|g_{f'_2 KK}|^2 = 19 \pm 3$  GeV $^{-2}$ . Since we lack experimental data to compare the amplitudes, we proceed to examining the trajectory. The parameters that we obtain are,

$$\alpha_0 = 0.53^{+0.10}_{-0.44}; \quad \alpha' = 0.63^{+0.20}_{-0.05} \text{ GeV}^{-2}; \quad b_0 = 1.33^{+0.63}_{-0.09}, \quad (14)$$

which give the Regge trajectory shown in Fig. 3. Again, we find the real part nearly linear and much larger than the imaginary part. As in the case of the  $f_2(1270)$ , the slope is compatible with that found for the  $P'$  trajectory in [1]  $\alpha'_{P'} \approx 0.83$  GeV $^{-2}$ , and the intercepts also agree.

As we did for  $f_2(1270)$ , we include in Fig. 3 the  $J = 4$  candidates for the  $f'_2(1525)$  trajectory. These are the  $f_J(2220)$  and the  $f_4(2300)$ . We remark that there is no experimental evidence of the  $f_4(2150)$  that was predicted in [1] from their analysis of the  $f'_2(1525)$  trajectory. As commented before, these resonances lie in a region, covered with a mesh in Fig. 3, beyond the strict applicability limit of our approach, where our results must be considered qualitatively at most.

Finally, we remark that the PDG list includes another  $f_2$  resonance, albeit requiring confirmation. It has a mass between that of the  $f_2(1270)$  and the  $f'_2(1525)$  and it could also have either the  $f_J(2220)$  or  $f_4(2300)$  as the higher mass partner.

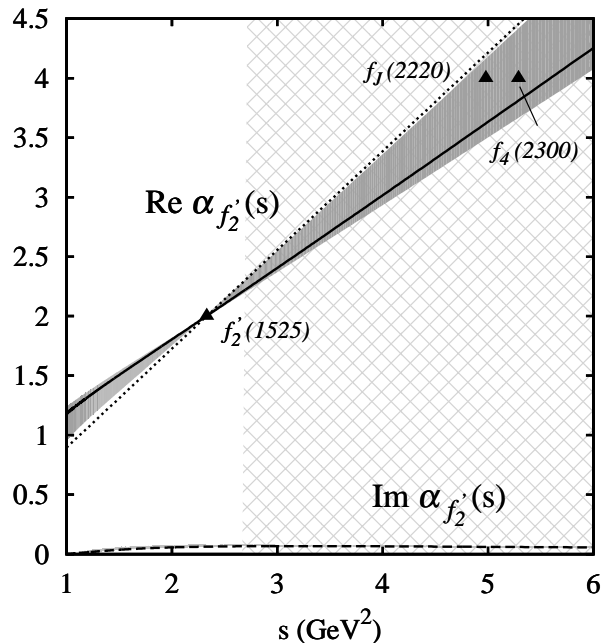


FIG. 3: Real (solid) and imaginary (dashed) parts of the  $f'_2(1525)$  Regge trajectory. The gray bands cover the uncertainties due to the errors in the input pole parameters and the area covered with a mesh is the mass region starting three half-widths above the resonance mass, where our elastic approach must be considered just as an extrapolation. For comparison, we show with a dotted line the Regge trajectory obtained in [1] and the resonances listed in the PDG that could belong to this trajectory.

#### IV. DISPERSION RELATION WITH THREE SUBTRACTIONS

As already mentioned in the introduction, one may wonder whether the linearity of the trajectories we obtain for the two D-wave resonances, as well as for the  $\rho(770)$  in [4], is related to use of two subtractions in the dispersion relation for  $\alpha(s)$ . In particular, since the resonances are rather narrow one could expect the imaginary part of their trajectories to be small, so that if the last term in Eq. (9) was dropped the trajectory would be reduced to a straight line. Thus, in order to show that the linearity of the trajectory is not forced by the particular parameterization, we repeated the calculations using three subtractions in the dispersion relations,

$$\text{Re } \alpha(s) = \alpha_0 + \alpha' s + \alpha'' s^2 + \frac{s^2}{\pi} PV \int_{4m^2}^{\infty} ds' \frac{\text{Im} \alpha(s')}{s'^2 (s' - s)}, \quad (15)$$

$$\text{Im } \alpha(s) = \frac{\rho(s) b_0 \hat{s}^{\alpha_0 + \alpha' s + \alpha'' s^2}}{|\sqrt{\Gamma(\alpha(s) + \frac{3}{2})}|} \exp \left( -\frac{1}{2} [1 - \log(\alpha'' s_0^2)] s (R + \alpha'' s) - Q s \right. \\ \left. + \frac{s^2}{\pi} PV \int_{4m^2}^{\infty} ds' \frac{\text{Im} \alpha(s') \log \frac{\hat{s}}{s'} + \frac{1}{2} \arg \Gamma(\alpha(s') + \frac{3}{2})}{s'^2 (s' - s)} \right), \quad (16)$$

with

$$R = B - \frac{1}{\pi} \int_{4m^2}^{\infty} ds' \frac{\text{Im} \alpha(s')}{s'^2}, \quad (17)$$

and

$$Q = -\frac{1}{\pi} \int_{4m^2}^{\infty} ds' \frac{-\text{Im} \alpha(s') \log \hat{s}' + \frac{1}{2} \arg \Gamma(\alpha(s') + \frac{3}{2})}{s'^2}. \quad (18)$$

The reason why the constants  $R$  and  $Q$  and the square root of  $\Gamma$  have been introduced is to ensure that, at large  $s$ ,  $\text{Im } \alpha(s)$  behaves as  $1/s$ . The parameters that we obtain for the trajectories with these dispersion relations are shown in Table I.

TABLE I: Parameters of the  $f_2(1270)$ ,  $f_2'(1525)$  and  $\rho(770)$  Regge trajectories using three-time-subtracted dispersion relations.

	$\alpha_0$	$\alpha'$ ( $\text{GeV}^{-2}$ )	$\alpha''$ ( $\text{GeV}^{-4}$ )	$b_0$
$f_2(1270)$	1.01	0.97	0.04	2.13
$f_2'(1525)$	0.42	0.65	0.02	4.58
$\rho(770)$	0.56	1.11	0.03	0.88

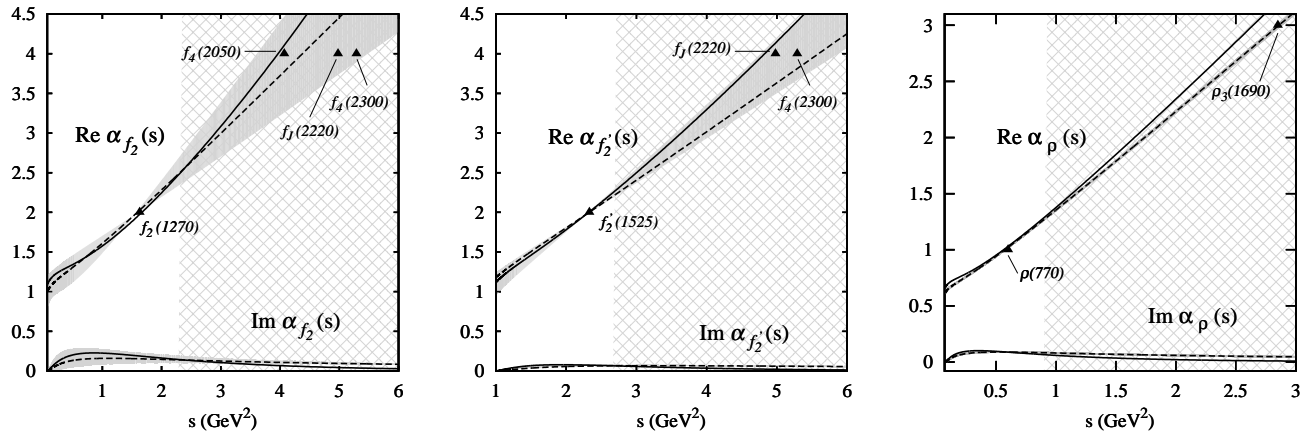


FIG. 4: Regge trajectories obtained using three-time-subtracted dispersion relations (solid lines) compared to the ones obtained with twice-subtracted dispersion relations (dashed lines with gray error bands).

With the above parameterization we obtain for the fitted pole parameters  $\sqrt{s_{f_2}} = 1267.3 - i90$  MeV,  $|g_{f_2\pi\pi}|^2 = 25$   $\text{GeV}^{-2}$ ,  $\sqrt{s_{f_2'}}$  = 1525 -  $i35$  MeV,  $|g_{f_2'\pi\pi}|^2 = 19$   $\text{GeV}^{-2}$ ,  $\sqrt{s_\rho} = 763 - i74$  MeV and  $|g_{\rho\pi\pi}|^2 = 35$   $\text{GeV}^{-2}$ . Therefore, despite having four parameters to fit three numbers, we find no real improvement in the description of the poles. In the case of three subtractions, neglecting the imaginary part of the resonances results in a quadratic trajectory. Therefore, in Fig. 4 we compare the trajectories using the three (solid line) and the two (dashed line) subtractions in the dispersion relations. We observe that in both cases there is a curvature, but that in the elastic region the trajectories are almost linear. The difference between the two methods only becomes apparent for masses well above the range of applicability. Moreover, the difference between the results obtained using two and three subtractions can be used as an indicator of the stability of our results and therefore confirms that the applicability range for our method is well estimated and ends as soon as the inelasticity in the wave becomes sizable.

## V. DISCUSSION, CONCLUSIONS AND OUTLOOK

In [4] a dispersive method was developed to calculate Regge trajectories of resonances that appear in the elastic scattering of two mesons. We showed how, using the associated scattering pole of the resonance it is possible to determine whether its trajectory is of a standard type, *i.e.* real and linear as followed by “ordinary”  $\bar{q}q$ -mesons, or not. This method thus provides a possible benchmark for identifying non-ordinary mesons. In particular the ordinary Regge trajectory of the  $\rho(770)$ , which is a well-established  $\bar{q}q$  state, was successfully predicted, whereas the  $\sigma$  meson, a long-term candidate for a non-ordinary meson, was found to follow a completely different trajectory.

In the first part of this work we have successfully predicted the trajectories of other two, well-established ordinary resonances, the  $f_2(1270)$  and  $f_2'(1525)$ . In particular, from parameters of the associated poles in the complex energy plane we have calculated their trajectories and have shown that they are almost real and very close to a straight line, as expected.

In the second part of this work we have addressed the question of whether choosing two subtractions in the dispersion relations of [4] was actually imposing that the real part of the trajectory is a straight line for relatively narrow resonances. To address this question we analyzed the same resonances using a dispersion relation with an additional subtraction. We have shown that within the range of applicability of our approach, which basically coincides with the elastic regime, the resulting trajectories are once again very close to a straight line.

In the future it will be interesting to use such dispersive methods to determine trajectories of other mesons *e.g.* the  $K^*(892)$  as well as the controversial “partner” the scalar  $K^*(800)$ , which is another long-time candidate for a non-ordinary meson. Heavy mesons in charm and beauty sectors can also be examined. We also plan to extend the method to meson-baryon scattering, where, for example, the  $\Delta(1232)$  is another candidate for an ordinary resonance. We are also extending the approach to coupled channels.

**Acknowledgments** We would like to thank M.R. Pennington for several discussions. JRP and JN are supported by the Spanish project FPA2011-27853-C02-02. JN acknowledges funding by the Fundación Ramón Areces. APS work is supported in part by the U.S. Department of Energy, Office of Science, Office of Nuclear Physics under contract DE-AC05-06OR23177 and DE-FG0287ER40365.

APS is supported in part by the U.S. Department of Energy under Grant DE-FG0287ER40365.

- 
- [1] A. V. Anisovich, V. V. Anisovich and A. V. Sarantsev, Phys. Rev. D **62**, 051502 (2000).
  - [2] P. Masjuan, E. Ruiz Arriola and W. Broniowski, Phys. Rev. D **85**, 094006 (2012).
  - [3] R. L. Jaffe, Phys. Rev. D **15**, 267 (1977); Prog. Theor. Phys. Suppl. **168**, 127 (2007). J. D. Weinstein and N. Isgur, Phys. Rev. Lett. **48**, 659 (1982); D. Black, A. H. Fariborz, F. Sannino and J. Schechter, Phys. Rev. D **59**, 074026 (1999). P. Minkowski and W. Ochs, Eur. Phys. J. C **9**, 283 (1999). J. A. Oller and E. Oset, Nucl. Phys. A **620**, 438 (1997) [Erratum-ibid. A **652**, 407 (1999)]. E. van Beveren and G. Rupp, Eur. Phys. J. C **22**, 493 (2001). J. R. Pelaez, Phys. Rev. Lett. **92**, 102001 (2004). J. Vijande, A. Valcarce, F. Fernandez and B. Silvestre-Brac, Phys. Rev. D **72**, 034025 (2005). J. R. Pelaez and G. Rios, Phys. Rev. Lett. **97**, 242002 (2006). F. Giacosa, Phys. Rev. D **74**, 014028 (2006). J. R. Pelaez, M. R. Pennington, J. Ruiz de Elvira, and D. J. Wilson, Phys. Rev. D **84**, 096006 (2011). T. Hyodo, D. Jido and T. Kunihiro, Nucl. Phys. A **848**, 341 (2010).
  - [4] J. T. Londergan, J. Nebreda, J. R. Pelaez and A. Szczepaniak, Phys. Lett. B **729**, 9 (2014) [arXiv:1311.7552 [hep-ph]].
  - [5] I. Caprini, G. Colangelo and H. Leutwyler, Phys. Rev. Lett. **96**, 132001 (2006) [hep-ph/0512364]. R. Garcia-Martin, R. Kaminski, J. R. Pelaez and J. Ruiz de Elvira, Phys. Rev. Lett. **107**, 072001 (2011) [arXiv:1107.1635 [hep-ph]].
  - [6] P.B.D Collins, *An Introduction to Regge Theory & High Energy Physics*. Cambridge University Press, Cambridge (1977). V. M. Gribov, *The Theory of Complex Angular Momenta*. Cambridge University Press, Cambridge (2003)
  - [7] P.D.B. Collins, R.C. Johnson, E.J. Squires, Phys. Lett. B **26**, 223 (1968).
  - [8] G. Epstein and P. Kaus, Phys. Rev. **166**, 1633 (1968); S. -Y. Chu, G. Epstein, P. Kaus, R. C. Slansky and F. Zachariasen, Phys. Rev. **175**, 2098 (1968).
  - [9] R. Garcia-Martin, R. Kaminski, J. R. Pelaez, J. Ruiz de Elvira and F. J. Yndurain, Phys. Rev. D **83**, 074004 (2011) [arXiv:1102.2183 [hep-ph]].
  - [10] K.A. Olive et al. (Particle Data Group), Chin. Phys. C, **38**, 090001 (2014).
  - [11] This resonance still “needs confirmation” and it is not yet known whether its spin is 2 or 4 [10].